Determination of multicanonical weight based on a stochastic model of sampling dynamics

Jae Gil Kim,[1,*] Yoshifumi Fukunishi,[2] Akinori Kidera,[3] and Haruki Nakamura[4]

[1]*Japan Biological Information Research Center (JBIRC), Japan Biological Informatics Consortium (JBIC), Aomi 2-41-6, Koto-ku, Tokyo, 135-0064, Japan*

[2]*Biological Information Research Center (BIRC), National Institute of Advanced Industrial Science and Technology (AIST), Aomi 2-41-6, Koto-ku, Tokyo, 135-0064, Japan*

[3]*Graduate School of Integrated Science, Yokohama City University, Yokohama 230-0045, Japan*

[4]*Laboratory of Protein Informatics, Research Center for Structural Biology, Institute for Protein Research, Osaka University 3-2 Yamadaoka, Suita, Osaka 565-0871, Japan*

(Received 4 March 2003; published 26 August 2003)

Based on the stochastic interpretation of the sampling process modeled by a Langevin equation, we present an effective iteration scheme to determine the weight in multicanonical molecular dynamics. Our method enables an automatic determination of the weight producing a uniform energy sampling via an iterative cancellation of the deterministic force in a Langevin equation. The deterministic force has been calculated from the energy trajectory by identifying the moments of the transition probability of a Fokker-Planck equation associated with a Langevin equation. The intimate relationship between the sampling process and the stochastic dynamics has been verified by applying the iteration scheme to a helix-coil transition of the 8-polyalanine system in a gas phase.

DOI: 10.1103/PhysRevE.68.021110 PACS number(s): 05.40.−a, 02.50.−r, 87.15.−v

I. INTRODUCTION

During the last decade, several sampling algorithms have been proposed to overcome quasiergodic problem occurring in the simulation of rough energy landscape [1–6]. Since the potential energy surfaces of the complex systems, such as protein folding [7], cluster melting [8], and spin glasses [9], are characterized by numerous local minima separated by high energy barriers, conventional Monte Carlo (MC) or molecular dynamics (MD) simulation fails to sample broad regions of thermally accessible phase space due to the trapping in one of the local energy basins. One effective way to alleviate this quasiergodicity is to modify the Boltzmann weight so that the simulation generates a random walk on the energy space, allowing the system to cross high energy barriers more frequently.

The multicanonical ensemble method [1] or an equivalent entropic sampling method [2] combined with MC simulation has been proved to be very effective in studying the first-order phase transitions of lattice spin systems [10] and folding problems of small peptide systems [11]. Recently, the multicanonical algorithm has been applied to MD by using a force scaling method in the constant temperature [12] and Nose-Hoover thermostat [13]. Once the multicanonical sampling is achieved with high statistics, the reweighting produces a canonical distribution at an arbitrary temperature with a considerable enhancement of the sampling efficiency [14]. In contrast to the canonical ensemble, the weight factor of the multicanonical ensemble is not known *a priori* and has to be determined by an iterative procedure since it is inversely proportional to the density of state, i.e., $\Omega(E)$. However, determination of the exact weight is very difficult and nontrivial for a complex system because of the exponential growth of the density of state with respect to the size of the system [16]. Therefore, it is very demanding to develop an efficient method to get the multicanonical weight.

In this paper, we propose one effective iteration scheme to determine the weight in multicanonical MD. Our method is based on the observation that the sampling process of MD can be considered as a stochastic diffusion on the energy space, which is modeled by a Langevin equation describing an overdamped Brownian motion [15]. Within the stochastic formulation the multicanonical sampling corresponds to a free Brownian motion whose dynamics is driven by only thermal fluctuations without any deterministic force. Thus, the iterative procedure modifying the weight is equivalent to the dynamical process approaching a free Brownian motion through an iterative cancellation of the deterministic force. Based on this analogy, a different iteration scheme has been developed for the derivative of the weight, which is identified with the deterministic force in our stochastic model. The iteration scheme has been further transformed to a recursive formula for the effective temperature, allowing an automatic calculation of the weight without any intervention in the simulation process.

The deterministic force plays a critical role in our stochastic formulation of the sampling process. In contrast to the conventional iteration scheme biasing the weight [12], our method utilizes a force biasing to attain the uniform sampling. In the present study, the deterministic force has been calculated by computing the drift and diffusion coefficients of a Fokker-Planck equation associated with a Langevin equation. We showed that the characteristic dynamics of the sampling process can be extracted from the time series data of MD by estimating the stochastic differential equation in the form of a Fokker-Planck equation. The performance of our method has been validated by applying it to a helix-coil transition of 8-polyalanine $[(\mathrm{Ala})_8]$ in a gas phase.

In Sec. II, the basic theory on the sampling process has

*Corresponding author. Email address: jgkim@jbirc.aist.go.jp

been discussed in terms of the stochastic differential equation (SDE). The physical implication of the proposed iteration scheme has been explained within the stochastic formulation. In Sec. III, the effectiveness of our method has been examined by using the multicanonical simulation of a helix-coil transition of the $(Ala)_8$ system. Detailed numerical results and discussions are presented with the stochastic interpretation of the sampling dynamics. The conclusion and a summary are added in Sec. IV.

II. THEORETICAL FORMULATION

A. Stochastic model of the sampling process

Let us start by briefly reviewing the conventional multicanonical ensemble method in MD. The uniform sampling in a multicanonical ensemble can be obtained by weighting each state of an energy E with weight $\mathcal{W}_{mc}$ [1,2] as

$$\mathcal{W}_{mc}(E)=1/\Omega(E)=e^{-\beta_0\alpha(E)}, \tag{1}$$

where $\beta_0=1/k_BT_0$ and $\alpha(E)$ is the multicanonical potential. In Eq. (1), the sampling of the multicanonical ensemble defined by weight $\mathcal{W}_{mc}$ has been considered as the canonical sampling associated with the effective potential $\alpha(E)$. Then, the energy trajectory in the multicanonical ensemble can be generated by performing the constant temperature MD at T_0 with a scaled Newton's equation [12]

$$\dot{\mathbf{p}}_i=-\frac{\partial\alpha(E)}{\partial\mathbf{q}_i}=\frac{\partial\alpha(E)}{\partial E}\mathbf{f}_i=\nu(E)\mathbf{f}_i, \tag{2}$$

where $\mathbf{q}_i$, $\mathbf{p}_i$, and $\mathbf{f}_i$ correspond to the coordinate, momentum, and force of the particle i on the original potential energy surface E, respectively. The derivative of the weight, i.e., $\nu(E)$ is the force scaling function characterizing the multicanonical ensemble. Since $\Omega(E)$ is not known *a priori*, the multicanonical potential $\alpha(E)$ has to be determined by using an iterative procedure with the update scheme of Ref. [12]:

$$\alpha^{i+1}(E)=\alpha^i(E)+\frac{1}{\beta_0}\ln P^i(E), \tag{3}$$

where α^i and P^i are the multicanonical potential and the energy distribution in the ith simulation, respectively. The simulation is iterated by substituting ν^{i+1} in Eq. (2) until the obtained $P(E)$ is reasonably flat within a certain energy range.

The SDE governing the sampling process in the multicanonical ensemble can be obtained by considering the probability density function (PDF) associated with weight $\mathcal{W}_{mc}$ as [15]

$$P(E)=\Omega(E)e^{-\beta_0\alpha(E)}/Z_\alpha=e^{-\beta_0A(E)}/Z_\alpha, \tag{4}$$

where $A(E)=\alpha(E)-T_0S(E)$, $S(E)$ being the microcanonical entropy defined by $k_B\ln\Omega(E)$. Here, Z_α is the partition function defined by $\int e^{-\beta_0A(E)}dE$. The PDF of Eq. (4) is obtained as a stationary solution of the Langevin equation of

$$\partial_tE=\Gamma(E)+\sqrt{k_BT_0}\,\eta(t), \tag{5}$$

where

$$\Gamma(E)=-\partial_EA(E)=1/\tilde{T}_S(E)-\nu(E) \tag{6}$$

and $\tilde{T}_S(E)=T_S(E)/T_0$, $T_S(E)$ being the statistical temperature defined in the microcanonical ensemble as $[\partial S/\partial E]^{-1}$ [21]. In Eq. (5), thermal fluctuations are approximated by an unbiased δ-correlated Gaussian white noise with $\langle\eta(t)\eta(t')\rangle=2\delta(t-t')$. The important observation in Eq. (5) is that the force scaling function in the modified Newton's equation is identified with the deterministic force driven by the weight in the Langevin equation. The deterministic force $\Gamma(E)$ has two contributions derived from the microcanonical entropy and the sampling weight. The former is the system-dependent quantity, which is not known *a priori*, but the effective force $\nu(E)$ can be adjusted by altering the multicanonical potential $\alpha(E)$. Our stochastic model reveals that the sampling process in the multicanonical ensemble can be considered as a stochastic diffusion on the free-energy potential $A(E)$ composed of the microcanonical entropy and the weight.

The uniform sampling can be realized from a generation of a random walk on the energy space when the deterministic force $\Gamma(E)$ becomes zero by the condition of $\alpha(E)=T_0S(E)$. Therefore, the iterative correction of $\alpha(E)$ with the update scheme of Eq. (3) is equivalent to the dynamical process of making $\Gamma(E)=0$. Our basic idea is that this iteration scheme can be made for the force scaling function by rearranging Eq. (6) as

$$\nu_S(E)=\nu(E)+\Gamma(E), \tag{7}$$

where $\nu_S(E)=1/\tilde{T}_S(E)$. If we estimate the deterministic part $\Gamma(E)$ from the simulation, Eq. (7) can be used to update the force scaling function. Since the trajectory in the multicanonical MD is directly related to the force scaling function, this iteration scheme is expected to be more effective than the conventional one updating the potential $\alpha(E)$. Denoting the stationary solution of Eq. (5), i.e., $P(E)=\exp[\beta_0\int^E\Gamma(E')dE']$, Eq. (7) can be also obtained by differentiating both sides of Eq. (3) as $\nu^{i+1}(E)=\nu^i(E)+k_BT_0\partial_E\ln P^i(E)$. However, it should be noted that the physical implication of Eq. (7) becomes transparent only in the stochastic formulation of the sampling process.

B. Determination of $\Gamma(E)$

The deterministic force plays a critical role in our stochastic formulation, since we employ the force biasing to obtain the uniform distribution in energy space contrary to the conventional potential biasing [12]. In our study, the deterministic force has been calculated by computing the stochastic components of the corresponding Fokker-Planck equation (FPE) as

$$\partial_tP=-\partial_ED^{(1)}(E)P(E,t)+\partial_E^2D^{(2)}(E)P(E,t), \tag{8}$$

where $D^{(1)}$ and $D^{(2)}$ correspond to the drift and diffusion coefficients. In the Ito interpretation, the coefficients of $D^{(1)}$ and $D^{(2)}$ correspond to the deterministic force Γ and $k_B T_0$, respectively [17]. When the dynamical process involves a few degrees of freedom, the stochastic components of the FPE can be estimated directly from the time series data of MD [18,19] as

$$D^{(k)} = \frac{1}{k!}\lim_{\Delta\to 0}\frac{\langle\{E(t+\Delta)-E(t)\}^k\rangle}{\Delta} = \frac{1}{k!}\lim_{\Delta\to 0}\frac{\langle X_k\rangle}{\Delta}, \tag{9}$$

where $\langle X_k\rangle$ denotes the conditional average of the energy increment at each time step subject to $E(t)=E$. The right-hand side of Eq. (9) is the moment of the transition probability density $W[E',t+\Delta|E,t]$ of the FPE, which is given by

$$W[X,E;\Delta] = \frac{1}{\sqrt{2\pi\sigma(\Delta)}}\exp\left\{-\frac{[X+Y(E)]^2}{2\sigma(\Delta)}\right\}, \tag{10}$$

where $X=E'-E$, $Y(E)=-\Gamma(E)\Delta$, and $\sigma(\Delta)=2D^{(2)}\Delta$ for an infinitesimal time interval Δ [15]. Then, by using the relation $\langle X_n\rangle=\int_{-\infty}^{\infty}X^n W[X,E]dX$, the first and second conditional averages of the transition probability are calculated as

$$\langle X_1\rangle = \Gamma(E)\Delta = D^{(1)}\Delta,$$

$$\langle X_2\rangle = \sigma(\Delta)+\langle X_1\rangle^2 = 2D^{(2)}\Delta+\Gamma(E)^2\Delta^2,$$

respectively. Notice that in the limiting of $\Delta\to 0$, $D^{(2)}$ approaches $\langle X_2\rangle/2\Delta$ as defined in Eq. (9). The second-order correction with respect to Δ in $\langle X_2\rangle$ represents an additional spreading of the probability flows due to the drift term besides thermal fluctuations. For a finite Δ, the estimate of $D^{(2)}$ becomes fairly bad if we ignore the second-order correction with respect to Δ in $\langle X_2\rangle$ [19]. With a few algebraic operations, the deterministic force is obtained by

$$\Gamma(E) = 2k_B T_0\frac{\langle X_1\rangle}{\langle X_2\rangle-\langle X_1\rangle^2}. \tag{11}$$

In actual computations, $\langle X_n\rangle$ are obtained by taking averages of the nth power of an energy increment $X=E'-E$ at each energy histogram E.

C. Effective temperature

The inverse of the force scaling function can be interpreted as a temperature scaling factor. For example, let us consider the constant force scaling function for a whole range of energy as $\nu(E)=1/\lambda$, λ being an arbitrary positive constant. Since $\alpha(E)=E/\lambda$ from the relation of Eq. (2), the probability density function of Eq. (4) reduces to the canonical PDF at the scaled temperature $T_0'=\lambda T_0$ as $P(E)\sim\Omega(E)e^{-\beta_0\alpha(E)}=\Omega(E)e^{-E/k_B T_0'}$. In the same limit, the Langevin equation reduces to

$$\partial_t E = -\xi(T_0')(E-E_0')+\cdots+\sqrt{k_B T_0}\,\eta(t) \tag{12}$$

by using the Taylor expansion of

$$\tilde{T}_S(E) = \lambda+\xi(T_0')(E-E_0')+\cdots,$$

where E_0' is determined by $\tilde{T}_S(E_0')=\lambda$ and $\xi(T_0')=1/(\lambda T_0')[\partial T_S/\partial E]_{E=E_0'}=[\lambda T_0' C_V(T_0')]^{-1}$, C_V being the specific heat of the system. Notice that E_0' becomes identical to an average energy at T_0' in a thermodynamic limit by the definition of $\partial_E S|_{E=E_0'}=1/T_0'$ [21]. Assuming that there is only one solution E_0' satisfying $\tilde{T}_S(E_0')=\lambda$, the first-order truncation of $\tilde{T}_S$ gives a typical canonical PDF of the Gaussian centered at E_0' with a width of $\sigma_0=k_B T_0'^2 C_V(T_0')$ as

$$P_0(E) = \frac{1}{\sqrt{2\pi\sigma_0}}\exp\left\{-\frac{(E-E_0')^2}{2\sigma_0}\right\}. \tag{13}$$

Therefore, by adjusting the value of λ, we can obtain the canonical sampling at an arbitrary temperature from the multicanonical simulation with a fixed T_0. It should be noted that the higher-order terms of $\tilde{T}_S$ have to be included in Eq. (12) when the relation of $\tilde{T}_S(E_0')=\lambda$ may not have a unique solution such as in the van der Waals loops of finite size system [20].

This interpretation can be extended to a continuous varying $\nu(E)$ by introducing the effective temperature $\tilde{T}(E)=1/\nu(E)$. Even though the original multicanonical sampling [1,2], i.e., the biasing of the weight to be coincided with $\Omega(E)$, has nothing to do with the temperature scaling, the concept of the effective temperature is very useful in explaining the essential dynamics of the multicanonical sampling. In the previous study [15], we showed that the uniform sampling in the multicanonical ensemble is achieved by transforming a complex free-energy surface into a piecewise multivalleyed landscape structure modulated by a stepwise effective temperature. In terms of the effective temperature, the multicanonial sampling can be considered as a repeated simulated annealing subject to an energy dependent heating and cooling schedule modulated by $\tilde{T}(E)$ [22]. The iteration scheme of Eq. (7) can be further transformed to a recursive formula for the effective temperature

$$\tilde{T}_S(E) = \frac{\tilde{T}(E)}{1+\Gamma(E)\tilde{T}(E)}. \tag{14}$$

Notice that $\tilde{T}_S(E)$ does not change for the energy region of $\Gamma(E)=0$, in which the sampling shows a random walk driven by only thermal fluctuations in Eq. (5). On the other hand, the effective temperature is iteratively modified for the force biased energy region of $\Gamma(E)\neq 0$.

A detailed procedure of our simulation scheme is outlined as follows.

(i) Perform the multicanonical simulation at an arbitrary temperature T_0 with an initial effective temperature $\tilde{T}^0(E)=1$ [$\nu^0(E)=1$].

(ii) By constructing the histogram of the energy difference X at each energy bin E, calculate the conditional averages of $\langle X_1 \rangle$ and $\langle X_2 \rangle$, and determine the ith deterministic force $\Gamma^i(E)$ using Eq. (11).

(iii) Update the effective temperature $\tilde{T}^{i+1}(E)$ using

$$\tilde{T}^{i+1}(E) = \begin{cases} \tilde{T}^i(E_1^i) & \text{for} \quad E \leqslant E_1^i \\ \dfrac{\tilde{T}^i(E)}{1+\Gamma^i(E)\tilde{T}^i(E)} & \text{for} \quad E_1^i \leqslant E \leqslant E_2^i \\ \tilde{T}^i(E_2^i) & \text{for} \quad E \geqslant E_2^i, \end{cases} \tag{15}$$

where E_1^i and E_2^i are the lowest and the highest energies sampled in the ith simulation.

(iv) Repeat steps (i)–(iii) for a certain number of iterations until the flat distribution is obtained. The multicanonical sampling with the update scheme of Eq. (15) shows characteristic sampling behaviors depending on the energy range. The sampling shows a typical random walk for $E_1^i \leqslant E \leqslant E_2^i$, since the deterministic force for that region has been canceled by $\Gamma^{i+1} = \nu^{i+1} - (\nu^i + \Gamma^i) = 0$. On the other hand, the dynamics generates the energy trajectories sampling the canonical ensembles of $\tilde{T}^i(E_1^i)$ and $\tilde{T}^i(E_2^i)$ in both ends of the sampling region, since the effective temperatures are constant for $E \leqslant E_1^i$ and $E \geqslant E_2^i$, respectively. It should be noted that the newly sampled energy trajectories in both ends will be used to estimate $\tilde{T}_S$ in the next iteration step. Thus, our multicanonical MD extends the sampling region via repeated exploratory canonical samplings in the boundary regions of $E \leqslant E_1^i$ and $E \geqslant E_2^i$.

III. NUMERICAL COMPUTATIONS AND DISCUSSIONS

A. Stochastic analysis of MD

To examine the performance of our method we applied it to a helix-coil transition of the $(\mathrm{Ala})_8$ system in a gas phase whose N and C termini were blocked with acetyl and *N*-methyl groups, respectively. The detailed characteristics of the helix-coil transition of the polyalanine system have been studied extensively using the multicanonical Monte Carlo simulations by Hansmann and co-workers [23]. Recently, the multicanonical MC has been further extended to larger systems beyond the small peptides [24]. In this study, MD simulation was performed by the program PRESTO [25] and the force-field parameters were taken from the all-atom version of AMBER [26] with a 1-fs time step, no cutoff, and SHAKE constraint. To show an applicability of Eq. (11), we first calculate $\Gamma(E)$ as a function of the reduced energy $(E - E_0)/\sigma_0$ for the canonical sampling at $T_0 = 300$ K. The PDF shows a typical Gaussian shape centered at the average energy E_0. The deterministic force represented by a solid line in Fig. 1(a) is greater (smaller) than zero for $E < E_0$ ($E > E_0$), which leads to a bias of the sampling toward E_0. The linear behavior of $\Gamma(E)$ around the average energy E_0 is a characteristic feature of the canonical sampling governed by the Ornstein-Uhlenbeck stochastic process [17]. But, we found that the deterministic force computed by Eq. (11) shows a slight deviation from dotted open square which is obtained by the derivative of the PDF. Even though the difference is small, the probability distribution might show a significant difference due to the accumulation of the bias in $\Gamma(E)$ as the iteration proceeds.

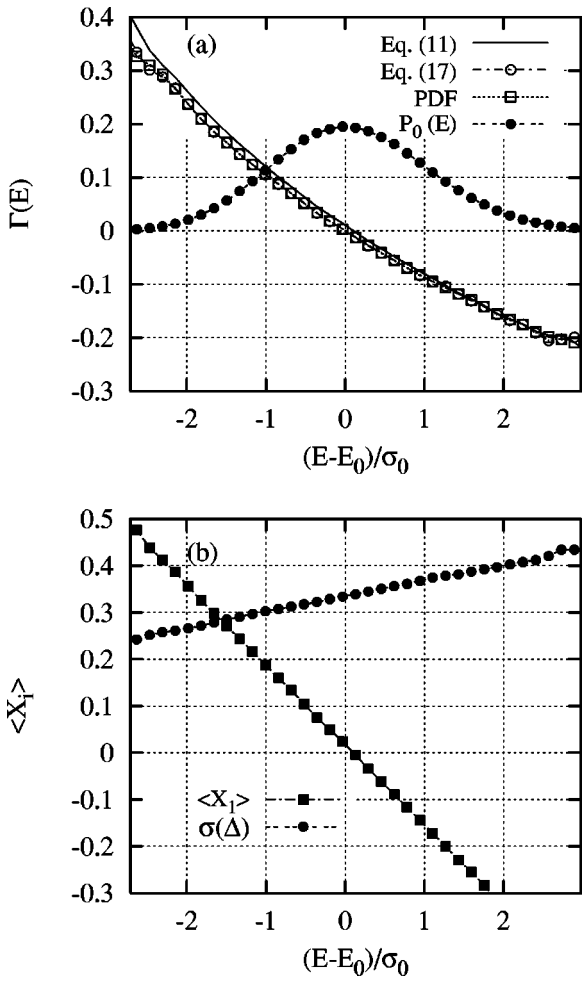

FIG. 1. (a) The deterministic forces $\Gamma(E)$ of the canonical sampling of $(\mathrm{Ala})_8$ in a gas phase at $T_0 = 300$ K. For comparison, the probability distribution is also plotted by dashed filled circles. $E_0 = 11.7$ kcal/mol and $\sigma_0 = 6.16$. (b) The conditional average $\langle X_1 \rangle$ and the variance $\sigma(\Delta)$ of the transition probability of Eq. (10).

This gives rise to a question about the validity of our basic assumption of Eq. (5). To check it we plot the conditional average $\langle X_1 \rangle$ and $\sigma(\Delta)$ for the same simulation data in Fig. 1(b), which are supposed to be $-\xi(T_0)\Delta(E - E_0)$ and $2k_B T_0 \Delta$, respectively, for a sufficiently small time step Δ in a canonical ensemble. If we assume that Δ is a constant as usual in MD, $\langle X_1 \rangle$ shows a consistent linear relationship with respect to the energy. But, $\sigma(\Delta)$ shows an energy dependence contrary to the expectation of our stochastic model. The energy dependence of $\sigma(\Delta)$ implies that the stochastic dynamics is driven by a multiplicative thermal noise. However, it should be emphasized that this problem is due to the size of the system, since the thermostat is not effective to produce a canonical ensemble in a small system. Actually, the value of $\sigma(\Delta)$ in a large system composed of $(\mathrm{Ala})_8$ in

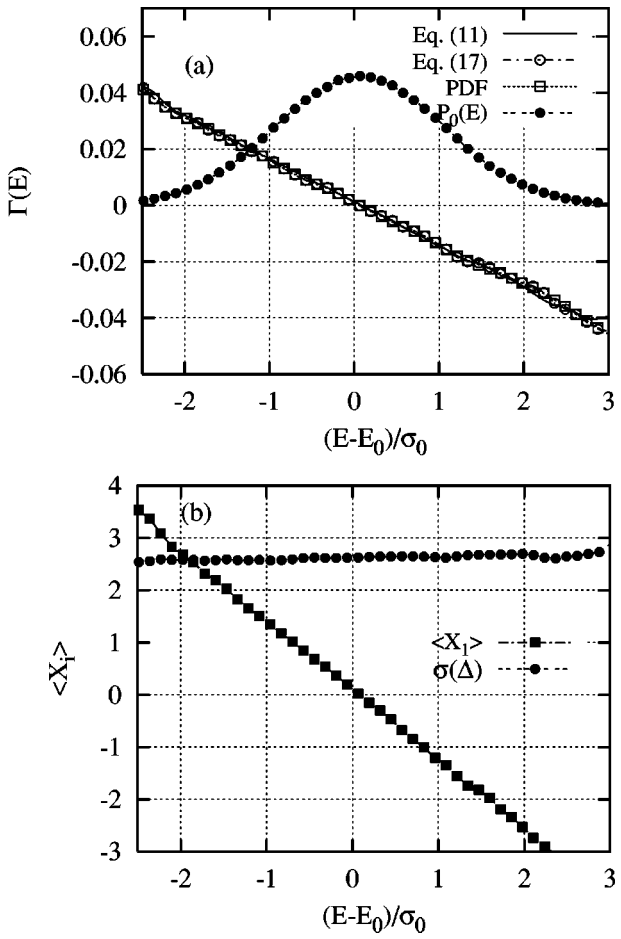

FIG. 2. (a) The deterministic forces $\Gamma(E)$ of the canonical sampling of $(\mathrm{Ala})_8$ in an explicit water phase at $T_0=300$ K. $E_0=-9140$ kcal/mol and $\sigma_0=78.4$ (b) The conditional average $\langle X_1 \rangle$ and the variance $\sigma(\Delta)$ of the transition probability.

explicit water molecules shows a constant behavior for statistically important energy range as in Fig. 2(b).

Our present formulation can be extended to include the stochastic process driven by a multiplicative noise as long as the sampling dynamics of MD obeys the Markov property. When the diffusion coefficient in the FPE is not constant, the stationary solution of Eq. (8) is given by

$$P_g(E)=N_0 e^{-\Phi(E)}, \tag{16}$$

where $\Phi(E)=\ln D^{(2)}(E)-\int^E dE'[D^{(1)}(E')/D^{(2)}(E')]$ and N_0 is a normalization constant [17]. Denoting $\Phi(E)=\beta_0 A(E)$, the deterministic force Γ is calculated as

$$\Gamma_g(E)=-\partial_E A=k_B T_0\left[\frac{D^{(1)}(E)}{D^{(2)}(E)}-\frac{D^{(2)\prime}(E)}{D^{(2)}(E)}\right], \tag{17}$$

where $D^{(1)}\Delta=\langle X_1 \rangle$, $D^{(2)}\Delta=(\langle X_2 \rangle-\langle X_1 \rangle^2)/2$, and $D^{(2)\prime}=\partial D^{(2)}(E)/\partial E$. Notice that if the diffusion coefficient $D^{(2)}$ is a constant, Eq. (17) reduces to Eq. (11). As can be seen in Fig. 1(a), the corrected Γ_g represented by dash-dotted open circles shows a perfect agreement with one obtained from the derivative of the PDF. In Fig. 2(a), we also plotted the deterministic forces differently calculated by Eqs. (11) and (17), and the derivative of the PDF for $(\mathrm{Ala})_8$ in an explicit water phase. The coincidence of $\Gamma(E)$ in Fig. 2(a) demonstrates that our basic assumption is indeed realized in a complex system. In actual simulation, Eq. (17) has been used to determine the deterministic force.

B. Multicanonical sampling based on the force biased iteration scheme

The advantage of this iteration scheme for the effective temperature is that it enables an automatic calculation of the weight without any intervention in the simulation. The trials to automatize the iteration procedures in the multicanonical ensemble have been also attempted in the Monte Carlo algorithm [27]. For the automatic iteration in MD, we updated the weight only for the restricted energy window $[E_1^i,E_2^i]$ defined by $P^i(E_1^i)=P^i(E_2^i)=0.005$ at each iteration step. For the energy region of $P^i(E)<0.005$, the deterministic force Γ^i has been assumed to be zero to handle the statistical error of small sampling data. The first update of the weight has been done after a 2×10^5 time step in the canonical MD at $T_0=300$ K. In the subsequent iterations, the number of sampling data has been increased to be $2(m+1)\times10^5$ time step, m being the iteration step, to maintain the statistical accuracy of the analysis for the extended sampling energy region.

The typical energy trajectory is plotted in Fig. 3(a). Starting from the canonical simulation at $T_0=300$ K the sampling is extended to cover an entire energy range as the iteration proceeds. The PDF of each iteration step has been also plotted in Fig. 3(b). The uniform distribution is obtained for an interesting energy region at $i=10$. To prevent the dynamics from trapping in local minima of low temperature energy region, the boundary condition of $\tilde{T}(E)=\tilde{T}(E_1^0)$ for $E<E_1^0=5$ kcal/mol has been applied. On the other hand, we set $\tilde{T}(E)=\tilde{T}(E_2^0)$ for $E>E_2^0=150$ kcal/mol. The conformational sampling has been checked by calculating the end-to-end distance d_l defined by the distance between N of $(\mathrm{Ala})_1$ and O of $(\mathrm{Ala})_8$. The broad distribution of d_l at $i=10$ confirms frequent transitions between the helix- and the random-coil state. The maximum peak locating at $d_l^\alpha\simeq14$ Å corresponds to the α helix state.

Except for the case of $i=3$, the deterministic force Γ^i shows two distinct behaviors depending on the energy range in Fig. 4(a). For the energy region of $[E_1^{i-1},E_2^{i-1}]$ sampled by the previous $(i-1)$th simulation, Γ^i becomes vanishing with the addition of the biasing force Γ^{i-1} to the previous force scaling function ν^{i-1}. Notice that $\Gamma(E)\simeq0$ for all energy ranges in final iteration of $i=10$. For the sampled energy region of $[E_2^{i-1},E_2^i]$ in the ith simulation, Γ^i shows a linear relationship with respect to the energy, which is a typical characteristic of the canonical sampling. In Fig. 4(b), both the force scaling function ν^i and the effective temperature $\tilde{T}^i$ are plotted with respect to E. The constant effective

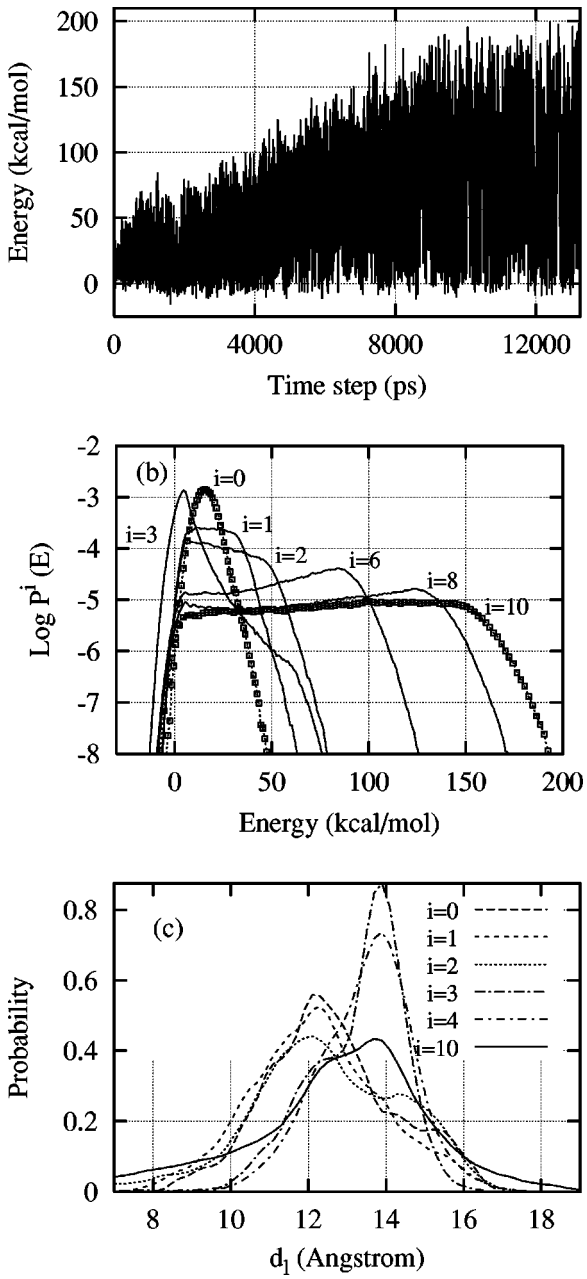

FIG. 3. (a) The energy trajectory with respect to a time step. (b) The probability distribution function $P^i(E)$ at each iteration step. (c) The distribution of the end-to-end distance d_l at each iteration step.

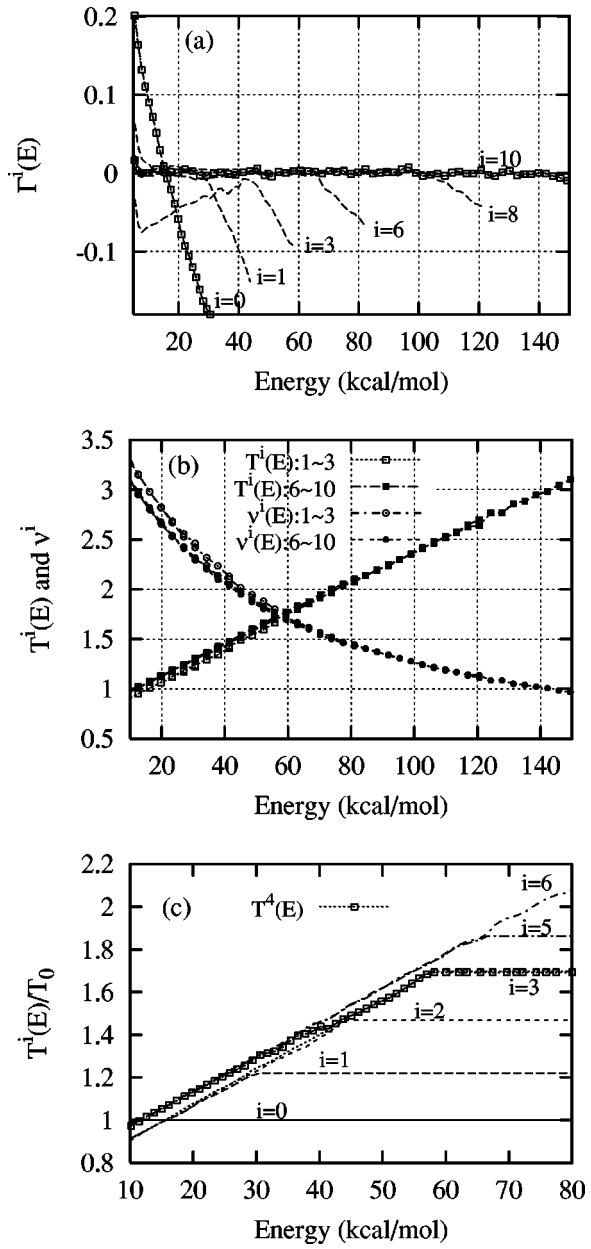

FIG. 4. (a) The deterministic force $\Gamma^i(E)$ as a function of the iteration i. (b) The force scaling function $\nu^i(E)$ and the effective temperature $\tilde{T}^i(E)$. (c) The magnified view of the effective temperature $\tilde{T}^i(E)$ for $i=0\sim6$.

temperature $\tilde{T}^0=1$ of the canonical sampling at $i=0$ transforms to the linear function of $\tilde{T}^1(E)=1/(1+\Gamma^0)\simeq 1-\Gamma^0(E)$, since Γ^0 is linear around the average energy. The effective temperature is repeatedly extended to high energy region through the subsequent transformations of

$$\tilde{T}^{i+1}(E)\simeq\tilde{T}^i(E_2^{i-1})-\Gamma^i(E), \tag{18}$$

where Γ^i is always negative for $[E_2^{i-1},E_2^i]$. Notice that $\tilde{T}^{i+1}(E)$ does not change significantly from $\tilde{T}^i$ for $E<E_2^{i-1}$, since $\Gamma^i\simeq 0$ for that energy region.

The interesting point is that the weight determined by the simulations of $i=0\sim2$ (dashed lines) does not coincide with the converged one (solid lines) obtained from $i=5\sim10$. This difference can be seen more clearly in a magnified view of the effective temperature in Fig. 4(c). The inconsistency of the weight is due to the quenching of the initial state, which has been prepared in a fully extended state of $(\mathrm{Ala})_8$ corresponding to $d_l=28.3$ Å. Notice that our simulation starts from the room temperature of $T_0=300$ K in contrast to very

high temperature of the conventional MUCA [11,12]. The rapid cooling of the initial state causes the system to be quenched in one of the local minima of the free-energy surface, which can be verified by the distinguished peak of $d_l^* = 12.1$ Å in the simulation of $i=0-2$ in Fig. 4(c). However, the system easily escapes from the quenched state by applying the biased force iteratively. The effective temperature $\tilde{T}^4$ connecting the initial weight to the converged one represents this transient dynamics. Also, the movement of the maximum peak of the end-to-end distance from d_l^* to d_l^α has been observed in this transient dynamics of $i=3$ of Fig. 3(c). The PDF and $\Gamma(E)$ associated with the transition show a strange behavior in Figs. 3(b) and 4(a), which do not coincide with the stochastic prediction. Indeed, the split of $\tilde{T}^i$ does not appear when we start the simulation from the well-defined equilibrium state of 300 K.

Once the multicanonical sampling is achieved with high statistics, the canonical PDF at an arbitrary temperature can be obtained by the reweighting as

$$P_0(E,T)=\Omega(E)e^{-\beta E}=P_{mu}(E)e^{\beta_0\alpha_{mu}(E)-\beta E}, \quad (19)$$

where P_{mu} and α_{mu} correspond to the PDF and the multicanonical potential at a final iteration, respectively. Furthermore, we can calculate various thermodynamics quantities of any physical observable O by

$$\langle O\rangle_T=\int dEO(E)P_0(E,T). \quad (20)$$

The reweighted PDF obtained from the multicanonical simulation at $i=10$ shows a good agreement with the canonical PDF at various temperatures in Fig. 5(a). We also plotted the reweighted average energy $\langle E\rangle_T$ with respect to the temperature in Fig. 5(b). In the previous study [15], we demonstrated that the multicanonical weight can be determined by interpolating the maximum probability energy points of the canonical samplings at different temperatures. Indeed, the reweighted average energy exactly coincides with the multicanonical weight $\tilde{T}^{10}$ in Fig. 5(b). In the present simulation, the maximum probability energy is identical to the average energy of each canonical sampling.

Finally, we would like to mention the scalability of the force biased iteration scheme with respect to the size of the system. We found that the convergence rate for the uniform sampling is not significantly different from the conventional potential biasing scheme in the present $(\mathrm{Ala})_8$ system. The uniform distribution has been obtained from the 11th iteration by applying the iteration scheme of Eq. (3). Since the convergence of the iteration depends on the system it is very difficult to derive a general relation quantifying the performance as a function of the size of the system. However, it should be emphasized that our method allows a full automatic determination of the weight without any intervention in the simulation process, which would be crucial in the performance as the size of the system increases.

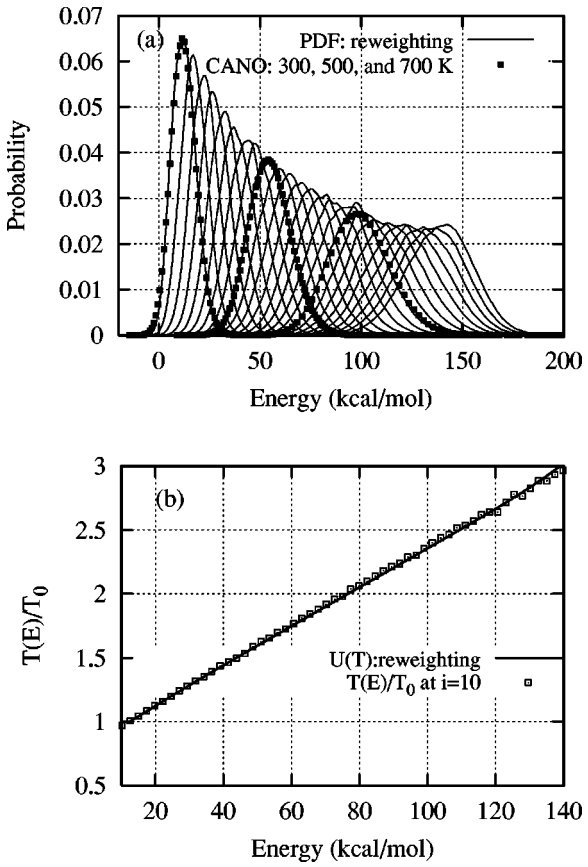

FIG. 5. (a) The solid lines represent the PDF determined by the reweighting of the multicanonical simulation at $i=10$. The temperature ranges from 300 K to 900 K with an increment 25 K. (b) The open squares and the solid line represent the effective temperature $\tilde{T}^{10}$ and the reweighted average energy $\langle E\rangle_T$, respectively.

IV. CONCLUSIONS

Based on the stochastic model of the sampling dynamics, we derive the iteration scheme for the derivative of the weight, which realizes the uniform sampling by canceling the deterministic force iteratively in a Langevin equation. The iteration scheme has been further transformed to give the recursive formula for the effective temperature, allowing full automatic calculation of the multicanonical weight without any intervention in the simulation. The essential dynamics of the sampling process has been verified in terms of the stochastic formulation of the time series data of MD by identifying the Fokker-Planck equation governing the dynamics. The validation of this iteration scheme has been tested in the multicanonical simulation of a helix-coil transition of the $(\mathrm{Ala})_8$ system.

ACKNOWLEDGMENTS

We thank M. S. Yukihisa Watanabe, Yoshiaki Mikami, and Takashi Kurosawa for technical supports. We acknowledge that this work was supported by the NEDO and the METI.

[1] B.A. Berg and T. Neuhaus, Phys. Lett. B **267**, 249 (1991).
[2] J. Lee, Phys. Rev. Lett. **71**, 211 (1993).
[3] D.D. Frantz, D.L. Freeman, and J.D. Doll, J. Chem. Phys. **93**, 2769 (1990).
[4] E. Marinari and G. Parisi, Europhys. Lett. **19**, 451 (1992); K. Hukushima and K. Nemoto, J. Phys. Soc. Jpn. **65**, 1604 (1996).
[5] J.P. Neirotti, F. Calvo, D.L. Freeman, and J.D. Doll, J. Chem. Phys. **112**, 10340 (2000).
[6] F. Wang and D.P. Landau, Phys. Rev. Lett. **86**, 2050 (2001).
[7] M. Karplus and G.A. Petsko, Nature (London) **347**, 631 (1990).
[8] J.P.K. Doye, D.J. Wales, and M.A. Miller, J. Chem. Phys. **109**, 8143 (1998).
[9] C. Maranas and C. Floudas, J. Chem. Phys. **97**, 7667 (1992).
[10] B.A. Berg and T. Celik, Phys. Rev. Lett. **69**, 2292 (1992).
[11] U.H.E. Hansmann and Y. Okamoto, J. Comput. Chem. **14**, 1333 (1993); Y. Sugita and Y. Okamoto, Chem. Phys. Lett. **314**, 141 (1999).
[12] N. Nakajima, H. Nakamura, and A. Kidera, J. Phys. Chem. B **101**, 817 (1997); U.H.E. Hansman, Y. Okamoto, and F. Eisenmenger, Chem. Phys. Lett. **259**, 321 (1996).
[13] S. Jang, Y. Park, and S. Shin, J. Chem. Phys. **116**, 4782 (2002).
[14] H. Shirai, N. Nakajima, J. Higo, A. Kidera, and H. Nakamura, J. Mol. Biol. **278**, 481 (1998); J. Higo, O.V. Galzitskaya, S. Ono, and H. Nakamura, Chem. Phys. Lett. **337**, 169 (2001).
[15] J.G. Kim, Y. Fukunishi, and H. Nakamura, Phys. Rev. E **67**, 011105 (2003).
[16] S. Kumar, P. Payne, and M. Vasquez, J. Comput. Chem. **17**, 1269 (1996); U.H.E. Hansmann, Phys. Rev. E **56**, 6200 (1997).
[17] H. Risken, *The Fokker-Planck Equation* (Springer, Berlin, 1984)
[18] R. Friedrich, J. Peinke, and Ch. Renner, Phys. Rev. Lett. **84**, 5224 (2000).
[19] M. Ragwits and H. Kantz, Phys. Rev. Lett. **87**, 254501 (2001).
[20] I.H. Umirazkov, Phys. Rev. E **60**, 7550 (1999).
[21] K. Huang, *Statistical Mechanics* (Wiley, New York, 1972).
[22] K.K. Bhattachaarya and J.P. Sethna, Phys. Rev. E **57**, 2553 (1998).
[23] Y. Okamoto and U.H.E. Hansmann, J. Phys. Chem. **99**, 11276 (1995); N.A. Alves and U.H.E. Hansmann, Phys. Rev. Lett. **84**, 1836 (2000).
[24] U.H.E. Hansmann and Y. Okamoto, J. Phys. Chem. B **103**, 1595 (1999); N.A. Alevs and U.H.E. Hansmann, J. Chem. Phys. **117**, 2337 (2002).
[25] K. Morikami, T. Nakai, A. Kidera, M. Saito, and H. Nakamura, J. Comput. Chem. **16**, 243 (1992).
[26] W.D. Cornell, P. Cieplak, C.I. Bayly, I.R. Gould, K.M. Merz, Jr., D.M. Ferguson, D.C. Spellmeyer, T. Fox, J.W. Caldwell, and P.A. Kollman, J. Am. Chem. Soc. **117**, 5179 (1995).
[27] F. Yasar, T. Celik, B.A. Berg, and H. Meirovitch, J. Comput. Chem. **21**, 1251 (2000); **23**, 1127 (2002).